Letters

A Double-Sided *LCLC*-Compensated Capacitive Power Transfer System for Electric Vehicle Charging

Fei Lu, *Student Member, IEEE*, Hua Zhang, *Student Member, IEEE*, Heath Hofmann, *Member, IEEE*, and Chris Mi, *Fellow, IEEE*

***Abstract*—A double-sided *LCLC*-compensated capacitive power transfer (CPT) system is proposed for the electric vehicle charging application. Two pairs of metal plates are utilized to form two coupling capacitors to transfer power wirelessly. The *LCLC*-compensated structure can dramatically reduce the voltage stress on the coupling capacitors and maintain unity power factor at both the input and output. A 2.4-kW CPT system is designed with four 610-mm × 610-mm copper plates and an air gap distance of 150 mm. The experimental prototype reaches a dc–dc efficiency of 90.8% at 2.4-kW output power. At 300-mm misalignment case, the output power drops to 2.1 kW with 90.7% efficiency. With a 300-mm air gap distance, the output power drops to 1.6 kW with 89.1% efficiency.**

***Index Terms*—Capacitive power transfer, electric vehicle charging, *LCLC* compensation.**

I. Introduction

CAPACITIVE power transfer (CPT) and inductive power transfer (IPT) are two effective methods to transfer power wirelessly [1]. The CPT technology utilizes high-frequency alternating electric fields to transfer power without direct electric connection, while the IPT system uses magnetic field to transfer power. The IPT technology has already been widely used in many applications, such as portable electronic devices, biomedical devices, and electric vehicle charging [2].

Manuscript received April 4, 2015; revised May 19, 2015 and June 7, 2015; accepted June 9, 2015. Date of publication June 17, 2014; date of current version July 10, 2015. This work was supported in part by the US Department of Energy Graduate Automotive Technology Education Grant; the US–China Clean Energy Research Center—Clean Vehicle Consortium, DENSO International, the University of Michigan–Dearborn, the University of Michigan–Ann Arbor, and China Scholarship Council.

F. Lu is with the Electrical Engineering and Computer Science Department, University of Michigan, Ann Arbor, MI 48109 USA, and also with the Department of Electrical and Computer Engineering, University of Michigan, Dearborn, MI 48128 USA (e-mail: feilu@umich.edu).

H. Zhang is with the Department of Electrical and Computer Engineering, University of Michigan, Dearborn, MI 48128 USA, and also with the School of Automation, Northwestern Polytechnical University, Xi'an 710072, China (e-mail: huazhang@umich.edu).

H. Hofmann is with the Electrical Engineering and Computer Science Department, University of Michigan, Ann Arbor, MI 48109 USA (e-mail: hofmann@umich.edu).

C. Mi is with the Department of Electrical and Computer Engineering, San Diego State University, San Diego, CA 92182-1309 (e-mail: mi@ieee.org).

Color versions of one or more of the figures in this paper are available online at http://ieeexplore.ieee.org.

Digital Object Identifier 10.1109/TPEL.2015.2446891

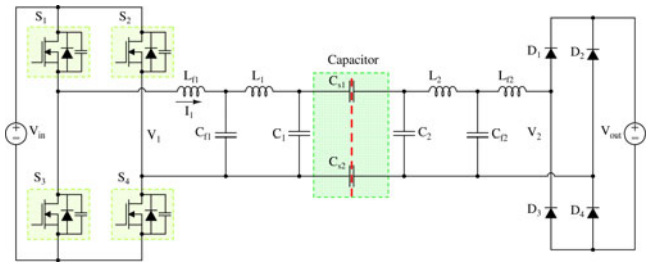

Fig. 1. Circuit topology of the proposed capacitive power transfer system.

Compared with the IPT system, the CPT system has many advantages. Magnetic fields are sensitive to nearby metal objects, and the system efficiency drops quickly with this interference [3]. They also generate eddy current losses and, hence, heat in a conductive object, which creates a potential fire hazard. However, the electric field in the CPT system does not generate significant losses in the metal objects.

The recent CPT system can be classified by the matching network topology. The most popular topology is a single inductor resonating with the capacitor to form a simple series-resonant circuit [4], [5]. The second topology is the *LCL* structure at the front-end to step-up the voltage for the coupling capacitor. However, there is also an inductor directly connected with the capacitor to form a series resonance [6]. In these two topologies, the series inductance is large because of the small value of capacitance. The voltage pressure on the capacitor is also large. The third topology is the resonant class E converter or the nonresonant PWM converter, used to replace the compensation inductor [7], [8]. All of these systems require very high-capacitance values, in the tens or hundreds of nanofarad range. So, the transferred distance is usually around 1 mm.

Compared with previous work [1], this paper focuses on 150-mm distance power transfer by capacitive coupling. It is designed for electric vehicle charging application. At this large distance, the coupling capacitance is typically in the picofarad range. The series-resonance topology is no longer suitable. In this paper, a double-sided *LCLC*-compensated topology as shown in Fig. 1 and its design process are proposed. Section II provides the circuit design procedure. Section III presents the capacitance simulation by Maxwell. Section IV designs a 2.4-kW prototype, and Section V validates the presented system by experiment. Section VI gives the conclusion.

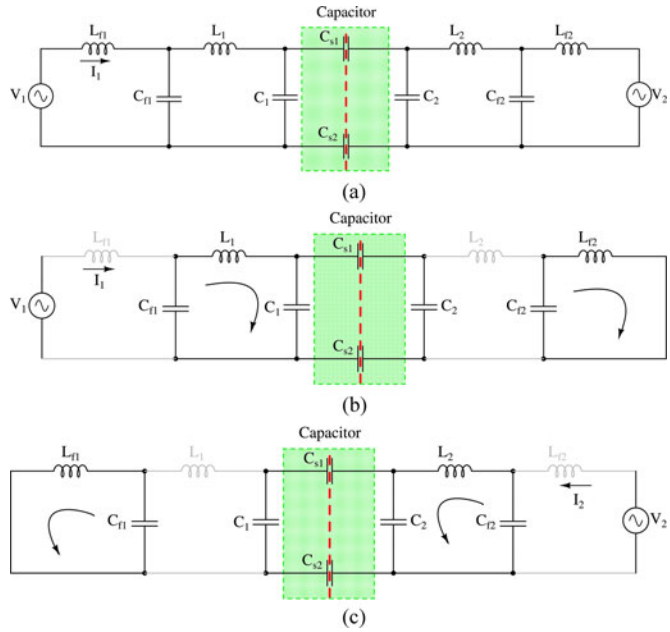

Fig. 2. Fundamental harmonic approximation analysis. (a) Simplifed resonant circuit topology. (b) Components excited by input voltage. (c) Components excited by output voltage.

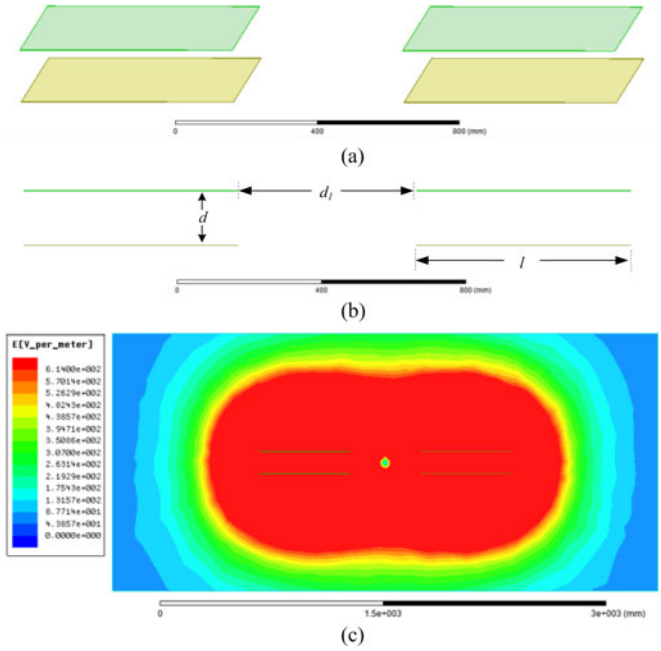

Fig. 3. Three-dimensional of the coupling capacitors. (a) Three-dimensional view of the capacitors. (b) Front view of the capacitors. (c) Electric-field strength around the plates.

II. Circuit Topology Design

A. LCLC Compensation Topology

Since the challenge in the CPT system is due to the small coupling capacitance value, the best solution is to connect an extra capacitor in parallel with the coupling capacitor. The *LCLC* network can help achieve unity power factor at both the input and output. The reactive power in the circuit is, therefore, eliminated and so the system efficiency is high.

B. Circuit Working Principle

The fundamental harmonic approximation method can be used to simplify the system, as shown in Fig. 2. Superposition theory can be used to analyze the circuit. Fig. 2(b) shows components excited by the input voltage at resonance. The circuit parameters are designed to achieve resonances at the same frequency. This shows that the input current is independent from the input voltage. Fig. 2(c) shows the components excited by the output voltage. Similarly, the output current does not depend on the output voltage. The parameter values should satisfy (1), where f_{sw} is the switching frequency

$$\begin{cases} L_{f1} = 1/(\omega_0^2 C_{f1}), L_{f2} = 1/(\omega_0^2 C_{f2}) \\ L_1 = 1/(\omega_0^2 C_{p1}) + L_{f1}, L_2 = 1/(\omega_0^2 C_{p2}) + L_{f2} \\ C_{p1} = C_1 + C_s \cdot C_2/(C_s + C_2), \\ C_{p2} = C_2 + C_s \cdot C_1/(C_s + C_1) \\ C_s = C_{s1} \cdot C_{s2}/(C_{s1} + C_{s2}), \omega_0 = 2\pi \cdot f_{sw}. \end{cases} \quad (1)$$

Fig. 2(b) shows that the output current leads the input voltage by 90°, and Fig. 2(c) indicates that the input current lags the output voltage by 90°. As an H-bridge rectifier is used at the output side, the output voltage and current are in phase. Therefore, the current and voltage are also in phase at the input side. As a result, the input power is expressed as

$$P_{\text{in}} = V_1 \cdot I_1 = \omega_0 C_s \cdot \frac{C_{f1} C_{f2}}{C_1 C_2 + C_1 C_s + C_2 C_s} \cdot V_1 \cdot V_2. \quad (2)$$

Since C_1 and C_2 are much larger than C_s, (2) can be approximated as

$$P_{\text{in}} = V_1 \cdot I_1 \approx \omega_0 C_s \cdot \frac{C_{f1} C_{f2}}{C_1 C_2} \cdot V_1 \cdot V_2. \quad (3)$$

III. Capacitance Analysis

Four metal plates were used to form two coupling capacitors to transfer power. Each plate size was selected as 24 in × 24 in (610 mm × 610 mm). The nominal distance d was 150 mm. The separation d_1 was set to be 500 mm to eliminate intercoupling between the two pairs of plates. The dimensions of the coupling capacitors are provided in Fig. 3(a) and (b).

Considering the edge effects [9], a single capacitor can be calculated as

$$C_{s1} = [1 + 2.343 \cdot (d/l)^{0.891}] \cdot (\varepsilon \cdot l^2/d) = 36.7 \text{ pF} \quad (4)$$

where $\varepsilon = 8.85 \times 10^{-12}$ F/m is the permittivity of free space.

Maxwell software from ANSYS is used to simulate a single capacitor at different misalignment and distance conditions. As shown in Fig. 4, the capacitance is not highly sensitive to misalignment and distance variations.

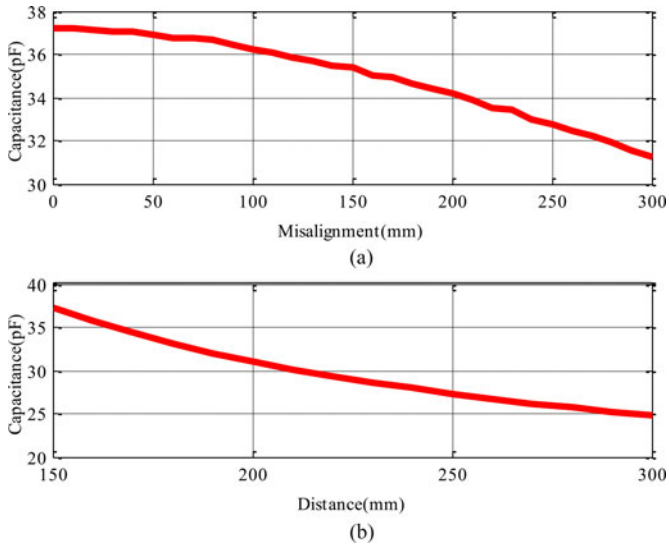

Fig. 4. Capacitance variations with misalignment and distance. (a) Capacitance at different misalignment. (b) Capacitance at different distance.

TABLE I
SYSTEM SPECIFICATIONS AND PARAMETER VALUES

V_{in}	V_{out}	f_{sw}	L_{f1} (L_{f1})	C_{f1} (C_{f2})	C_1 (C_2)	L_1	V_2
265 V	280 V	1 MHz	11.6 μH	2.18 nF	100 pF	231μH	242 μH

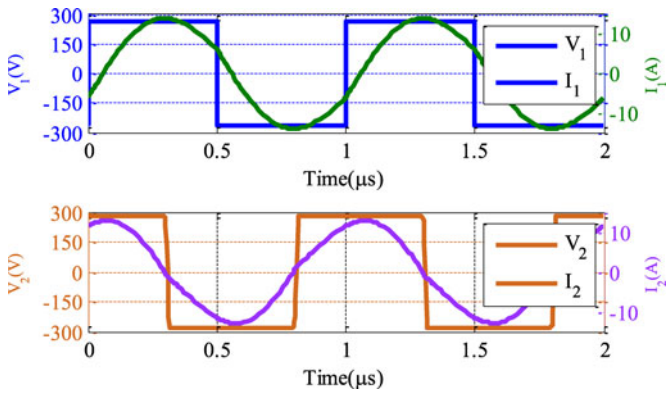

Fig. 5. LTSpice simulation of input and output waveforms.

IV. 2.4-kW CPT System Design

A 2.4-kW CPT system is designed using the procedure in Section II. The system parameters are shown in Table I.

It needs to be emphasized that the inductor L_2 is designed to be 5% larger than L_1 to achieve zero-voltage turn-on for the input inverter. Fig. 5 shows the simulated input and output waveforms.

The LT Spice-simulated output power is 2.4 kW, which is the desired value. Fig. 5 shows that the input current is positive at the turn-on transient, which means the body diode conducts current. Therefore, the switching loss is reduced. Table II shows the components' peak voltage/current stress.

TABLE II
PEAK VOLTAGE/CURRENT STRESS ON COMPONENTS

Components	L_{f1} (L_{f2})	C_{f1} (C_{f2})	C_1 (C_2)	L_1 (L_2)	*Plates*
Voltage	1.0 kV	1.0 kV	7.2 kV	7.2 kV	3.2 kV
Current	15.5 A	15.0 A	4.8 A	5.2 A	0.7 A

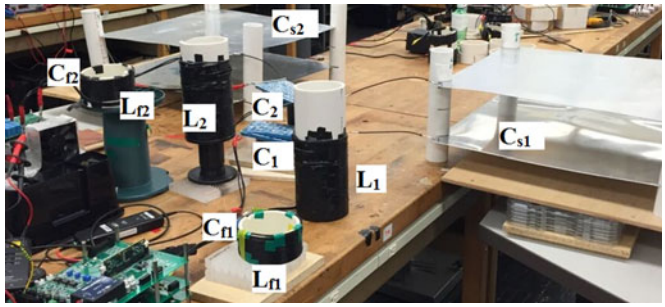

Fig. 6. 2.4-kW prototype of CPT system.

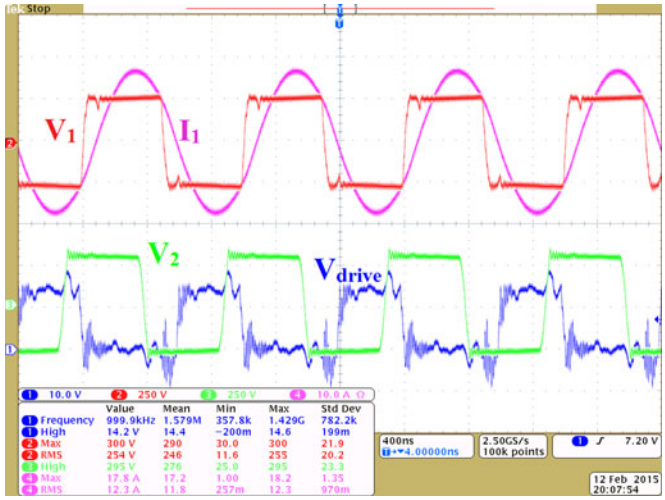

Fig. 7. Experiment waveform of CPT system.

Fig 3(c) shows the Maxwell simulation result of the electric field strength. According to IEEE standard [10], the safe area for this system is about 0.6 m away from the plates, where the field strength is lower than 614 V/m.

V. Experiment

Using the parameters in Table I, a 2.4-kW prototype was constructed, as shown in Fig. 6. Four 610-mm × 610-mm aluminum plates were used to form two capacitors and the nominal distance is 150 mm. Table II shows that the peak voltage is 3.2 kV. Since the breakdown voltage of air is approximately 3 kV/mm, there is no concern with arcing. For capacitors C_1 and C_2, ten film capacitors with 2000-V dc voltage rating are connected in series. The inductors are wound in multiturn shapes, so the voltage pressure between turns is limited and the insulation between turns can prevent arcing.

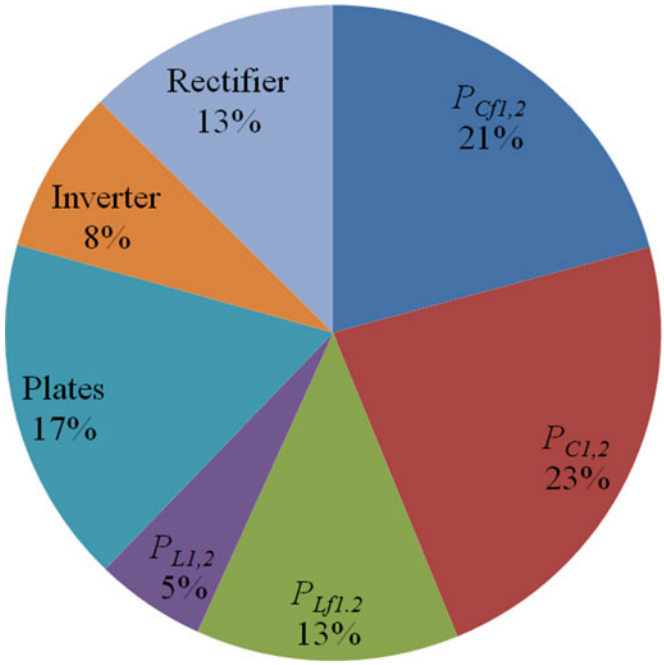

Fig. 8. Power loss distribution of each component.

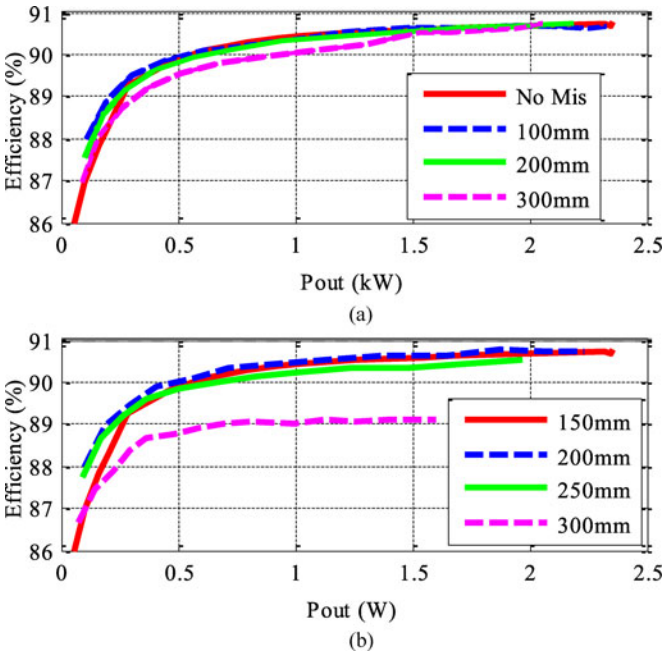

Fig. 9. System performance under different conditions. (a) Output power and efficiency at different misalignments. (b) Output power and efficiency at different distances.

Experimental results are shown in Fig. 7. The zero-voltage turn-on is achieved at the input side and the waveform is similar to the simulation in Fig. 5. The output power is 2.4 kW with 90.8% efficiency at 150 mm distance and no misalignment. The power loss on components can be estimated by the parasitic resistance of the component and also the current stress in Table II. The power loss distribution is shown in Fig. 8. Future research will focus on system optimization to minimize losses and increase efficiency.

The system performance at different conditions is provided in Fig. 9. It shows that the CPT system can maintain 2.1-kW output with 90.7% efficiency at 300-mm misalignment. Also, it can maintain 1.6-kW output with 89.1% efficiency at 300-mm distance. So the CPT system is robust to misalignment and distance variations compared to IPT systems.

VI. Conclusion

This paper proposes an *LCLC*-compensated topology for capacitive power transfer, which can deliver several kilowatt of power with a dc–dc efficiency higher than 90% through a distance of 150 mm. The system design procedure is provided and a 2.4-kW prototype is built. The experimental results validate the circuit topology. The CPT system is robust to misalignment and distance variations. Future research will include FEA simulations of electric fields, electromagnetic interference, electric-field shielding, safety, and power-loss minimization.

References

[1] J. Dai and D. Ludois, "A survey of wireless power transfer and a critical comparison of inductive and capacitive coupling for small gap applications," *IEEE Trans. Power Electron.*, vol. PP, no. 99, pp. 1–1, doi: 10.1109/TPEL.2015.2415253

[2] S. Li, W. Li, J. Deng, and C. C. Mi, "A double-sided LCC compensation network and its tuning method for wireless power transfer," *IEEE Trans. Veh. Technol.*, vol. 64, no. 6, pp. 1–12, Jun. 2015.

[3] D. J. Graham, J. A. Neasham, and B. S. Sharif, "Investigation of methods for data communication and power delivery through metals," *IEEE Trans. Ind. Electron.*, vol. 58, no. 10, pp. 4972–4980, Oct. 2011.

[4] C. Liu, A. P. Hu, G. A. Covic, and N. C. Nair, "Comparative study of CCPT systems with two different inductor tuning positions," *IEEE Trans. Power Electron.*, vol. 27, no. 1, pp. 294–306, Jan. 2012.

[5] D. C. Ludois, M. J. Erickson, and J. K. Reed, "Aerodynamic fluid bearing for translational and rotating capacitors in noncontact capacitive power transfer systems," *IEEE Trans. Ind. Appl.*, vol. 50, no. 2, pp. 1025–1033, Mar./Apr. 2014.

[6] M. P. Theodoridis, "Effective capacitive power transfer," *IEEE Trans. Power Electron.*, vol. 27, no. 12, pp. 4906–4913, Dec. 2012.

[7] D. Schmilovitz, A. Abramovitz, and I. Reichman, "Quasi resonant LED driver with capacitive isolation and high PF," *IEEE J. Emerg. Sel. Topics Power Electron.*, vol. PP, no. 99, pp. 1–1 doi: 10.1109/JESTPE.2015.2419882

[8] J. Dai and D. C. Ludois, "Single active switch power electronics for kilowatt scale capacitive power transfer," *IEEE J. Emerg. Sel. Topics Power Electron.*, vol. 3, no. 1, pp. 315–323, Mar. 2015.

[9] H. Nishiyama and M. Nakamura, "Form and capacitance of parallel-plate capacitor," *IEEE Trans. Compon. Packag. Manuf. Tech. A*, vol. 17, no. 3, pp. 477–484, Sep. 1994

[10] *IEEE Standard for Safety Levels With Respect to Human Exposure to Radio Frequency Electromagnetic Fields, 3 kHz to 300 GHz*, IEEE Standard C95.1, 2005.